Preliminary Evaluation of Robotic Needle Distal Tip Repositioning

Conor J. Walsh*[ab], Alexander H. Slocum[b], Rajiv Gupta[a]
[a]Dept. of Radiology, Massachusetts General Hospital, Boston, MA 02114; [b]Dept. of Mechanical Engineering, Massachusetts Institute of Technology, Cambridge, MA 02139

ABSTRACT

Advances in medical imaging now provide detailed images of solid tumors inside the body and miniaturized energy delivery systems enable tumor destruction through local heating powered by a thin electrode. We have developed a robot for accurately repositioning the distal tip of a medical instrument such an ablation probe to adjacent points within tissue. The position accuracy in ballistics gelatin was evaluated in a 2D experimental setup with a digital SLR camera that was fixed to a rig that also contained the gelatin. The robot was mounted to the rig in such a way that the stylet was deployed in a plane parallel the camera's lens. A grid paper attached to the back of the box containing the gelatin provided a stationary reference point for each of the pictures taken and also served as a coordinate system for making measurements. The measurement repeatability error was found by taking a stylet tip position measurement five times for two different pictures and found to be 0.26 mm. For a stylet with a radius of curvature of 31.5 mm and a diameter of 0.838 mm, the targeting accuracy was found to be 2.5 ± 1.4 mm at points that were approximately 38 mm lateral from the cannula axis.

Keywords: robot, steering, ablation, computed tomography, image-guided

1. INTRODUCTION

Dot-matrix printers allow a detailed 2D image on a computer screen to be precisely converted to a physical representation through a discrete set of small dots. In a similar way, computer controlled machining (CNC) is the execution of a machining plan from a computer aided design package for the creation of a three dimensional part. This paper focuses on the preliminary evaluation of a compact medical robot that is intended to be directly coupled to medical imaging systems so that information on tumor geometry and location can be used for more accurate diagnosis and treatment of disease.

In medicine there is an increasing shift away from open surgical procedures and towards minimally invasive approaches. This is due to advances in imaging and is resulting in reduced trauma and recovery time for patients. Miniature cameras and light sources placed inside the body via small incisions and natural orifices are enabling endoscopic and laparoscopic surgery where doctors manipulate surgical tools while viewing their motion. Imaging techniques such as ultrasound and optical coherence tomography allow doctors to visualize the extent of pathology below the skin surface. Whole body imaging modalities such as computed tomography (CT) and magnetic resonance imaging (MRI) provide highly detailed maps of patient anatomy and are becoming the workhorses of hospitals for diagnosis, treatment and follow-up.

1.1 Thermal Ablation

Another factor driving less invasive therapy is the development of treatment systems based on local energy delivery. Instead of the surgeon using a cold scalpel to open up a patient and cut out a tumor, a growing number of cases can now be treated through local heating or cooling. These techniques are referred to as thermal ablation and over 40,000 solid tumor ablations were performed in the US last year (estimated 140,000 worldwide) and this is projected to grow at an annual rate of 12% [1]. These procedures are often performed under image-guidance and are extremely dependent upon exact probe positioning.

Further author information:
Conor J. Walsh: E-mail: walshcj@mit.edu, Telephone: +1 617 780-9915

Energy-based Treatment of Tissue and Assessment VI, edited by Thomas P. Ryan, Proc. of SPIE Vol. 7901
790108 · © 2011 SPIE · CCC code: 1605-7422/11/$18 · doi: 10.1117/12.876604

Radiofrequency (RF) ablation remains the most widely used thermoablative technique worldwide. RFA of lung tumors was first described in animal tumor models in 1995 [2] and reported in patients in 2000 [3]. The main criticisms of RF ablation for cancer treatment have focused on the high local recurrence rates, in particular in the treatment of masses larger than 3 cm in diameter [4, 5] and the potential for incomplete tumor ablation near blood vessels because of the heat sink effect of local blood flow [6]. Lee et al. treated 32 malignant lung masses (27 NSCLC and five metastasis) with CT-guided RFA and found that lung cancers smaller than 3 cm had a higher necrosis rate when compared with large tumors (100% vs. 23%) [4]. This is primarily because the current probes provide a static and relatively small volume of coagulative necrosis that limits their ability to treat large or irregularly shaped tumors. In the lung, the size of burn volumes created by RF ablation is limited due to the high impedance environment created by the aerated tissue and smaller amounts of water compared to solid organs [7]. The consequence for patients is a failure to destroy all of a tumor as shown in Figure 1.

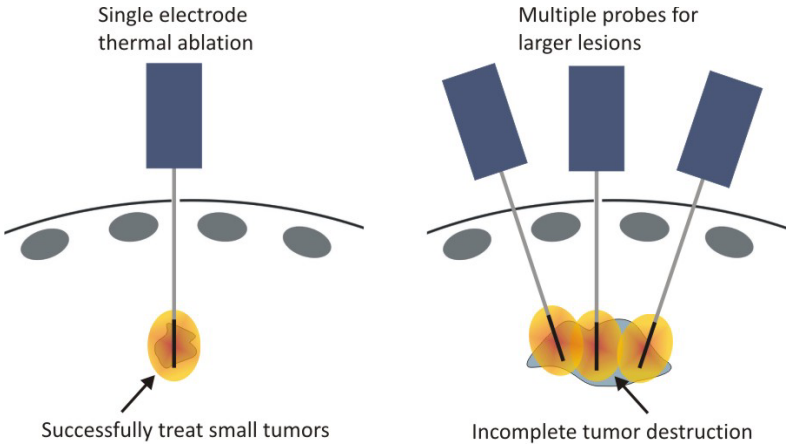

Figure 1. Left; the small burn volume associated with a single radiofrequency ablation probe is shown. While the temperature at the tip is 100°C (cannot exceed this because boiling occurs), it drops off rapidly and thus does not destroy the entire tumor. Right; an attempt is made to ablate a larger tumor with three ablation probes; however because planning and placement is currently performed manually, this often results in incomplete tumor ablation as illustrated.

To ablate large tumors, radiologists currently try to cover the arbitrarily shaped tumor with a given number of discrete objects of approximately known shape, representing the critical ablation temperatures for killing cancerous cells. Unfortunately, it is very difficult to find the optimal treatment plan when the radiologists have to rely on 2D-slices. However, precise and accurate deployment of multiple probes, which is required to execute the treatment plan, is still difficult to achieve in practice because probe placement is manual and accuracy is limited.

1.2 Image-Guided Medical Robots and Steerable Needles

A more recent advancement in the field of image-guided interventions has been the development of medical robots that integrate with CT or MRI machines. By coupling the precise positional information from the imaging systems, more accurate and efficient interventional procedures can be performed by the robots. These robots are mounted on the CT scanner bed [8-10] or the patient [11-13] and provide some method for remote needle orientation and insertion. The majority of these manipulators provide a remote center of rotation so that the needle can pivot about the skin surface [14-16]. More recently researchers have developed needle steering robots for controlling the trajectory as it is inserted into tissue. The two main strategies that have been employed to achieve steering are utilizing asymmetric forces at the needle tip (e.g. due to bevel) [17-19] or rotation and translation of concentric pre-curved tubes [20, 21] [22] [23, 24]. A subset of the concept of full six-degree-of-freedom needle steering using concentric pre-curved tubes is a superelastic pre-curved stylet combined with a stiffer concentric outer cannula. Two commercially available, passive devices for spinal procedures, such as vetebroplasty, are based on this concept and are intended for procedures where a target cannot be reached along a straight path [25, 26].

1.3 Contribution

Using this concept of a pre-curved stylet and straight concentric cannula, our team has built a telerobot that automates translation and rotation of the cannula and translation of the stylet with respect to it. Actuation of these three degrees-of-freedom enables repositioning the distal tip of the stylet to adjacent points in a volume as illustrated in Figure 2.

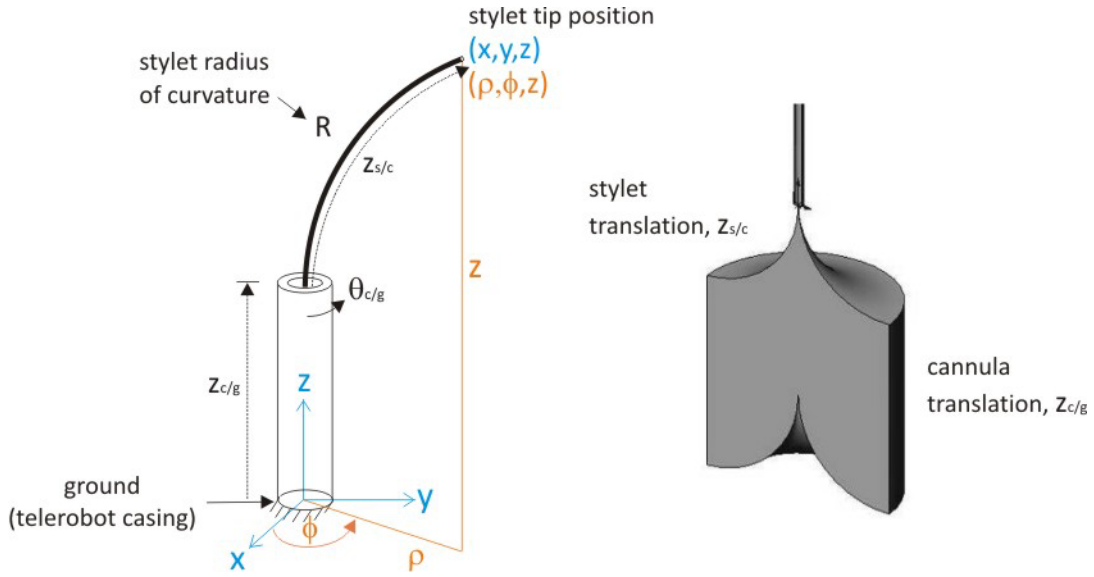

Figure 2. Left, coordinate system and position variables for cannula and stylet. In order to position the distal tip of the stylet in a volume then three degrees of freedom have to be controlled; $z_{c/g}$, the axial position of the cannula with respect to ground (i.e. the casing); $\theta_{c/g}$, the angle of rotation between the cannula and the casing and $z_{s/c}$, the axial position of the stylet with respect to the cannula. Right, illustration of the volume can be targeting through these degrees of freedom.

The particular focus of this paper is on the preliminary evaluation of this concept in a bench level setup using a block of ballistics gelatin and a digital SLR camera. The actual stylet tip position is predicted with a kinematic model and compared to the experimental data to evaluate the positioning capability of the device.

2. ROBOTIC NEEDLE STEERING INSTRUMENT

The detailed design of the robot will be described in a later paper but was designed to be constructed largely of plastic components so that it could be compatible with computed tomography imaging. Furthermore, strong emphasis was placed on developing a compact and cost-effective device that would have the potential to be clinically adopted.

2.1 Mechanism Description

The robotic mechanism is shown Figure 3. The device has a protruding cannula and a stylet with a curved distal tip pre-assembled inside. Inside the cylindrical plastic casing, the proximal end of the cannula is attached to the distal end of a hollow screw-spline and the proximal end of the stylet is attached to the distal end of a screw that fits inside the screw-spline. Each attachment is achieved via aluminum threaded inserts that are bonded to the proximal end of the shafts. The length of the cannula and stylet were chosen so as to be positioned at the distal tip of a 10 cm access cannula when the parts are connected via a standard medical leur-lock. The positioning accuracy and range of motion for the robotic mechanism were chosen such that the cannula could be rotated a full 360° in degree increments, the cannula could be translated with respect to the casing in millimeter increments and the stylet could be translated relative to the cannula in millimeter increments also.

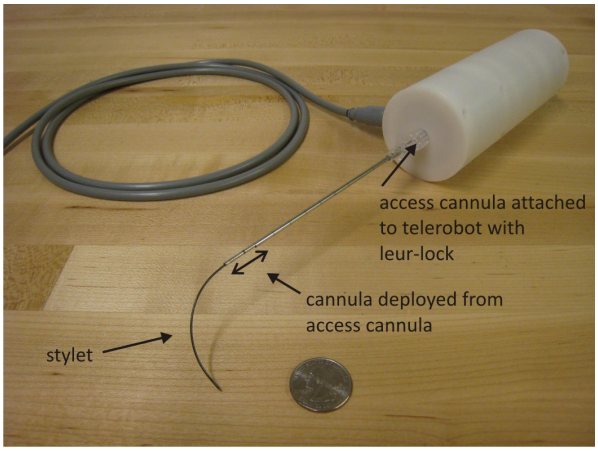

Figure 3. Prototype of the telerobot shown attached to an access cannula via a standard medical leur-lock. The stylet is shown in its deployed position and the cannula is protruding about 1 cm from the distal tip of the access cannula. A quarter is shown for scale.

2.2 Intended Mounting

The robotic mechanism was designed to be a compact modular end-effector that could be either attached to an access cannula that is first placed using a patient-mounted robot such as [13] or could be placed using a robotic manipulator arm (e.g. Neuromate Neuro Surgical Robot, Renishaw, UK) as illustrated in Figure 4. If connected to an access cannula it was desirable that this would be via a standard medical connector such as a leur-lock connector. This approach could enable the system to be used within the size constraints of a medical imaging system as the overall height requirement is reduced by first placing the access cannula. However, if placed manually, a means of supporting the mass of the access cannula and the telerobot would be required.

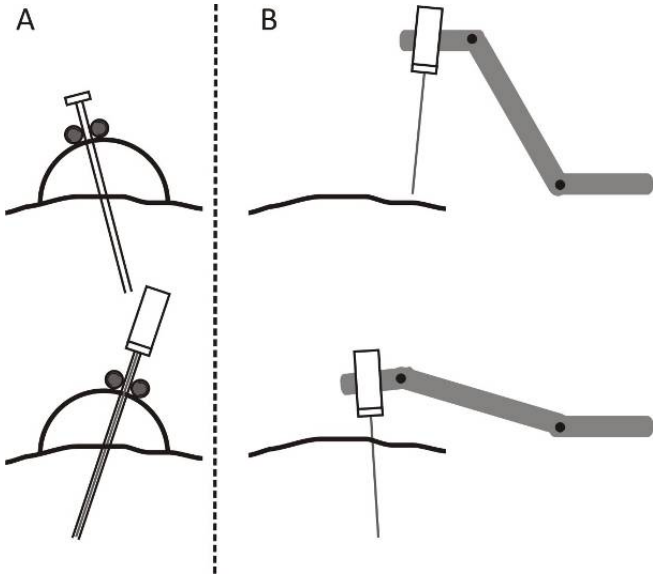

Figure 4. Strategies for application of the needle steering system. In (A), the telerobot is attached to a previously inserted access cannula. In (B), the needle steering system is attached to a robot arm.

3. TARGETING EXPERIMENTS

While, the intended use for the device is to achieving accurate targeting in three dimensions, an experimental test apparatus and methodology was developed to enable an initial evaluation of the positioning accuracy in 2D in ballistics gelatin in a lab bench-top environment.

3.1 Experimental Setup

A custom fixture was constructed for aligning and securing a digital SLR camera and a box of ballistics gelatin. The rig included a long plate specifically designed for the dimensions of the gel box rig and the Nikon D80 DSLR camera. Tapped holes were included in the plate to allow the gel box rig to be screwed into the plate. On the other end, mounting holes for the camera and alignment screws were placed at 1 inch increments to allow for multiple camera positions and room for focus length adjustments. The camera was fixed to the plate using the same ¼-20 screw hole that would normally be used to mount the camera to a tripod. The alignment screws act to align the camera such that pictures are taken with the lens parallel to the gel box. The experimental setup is shown in Figure 5.

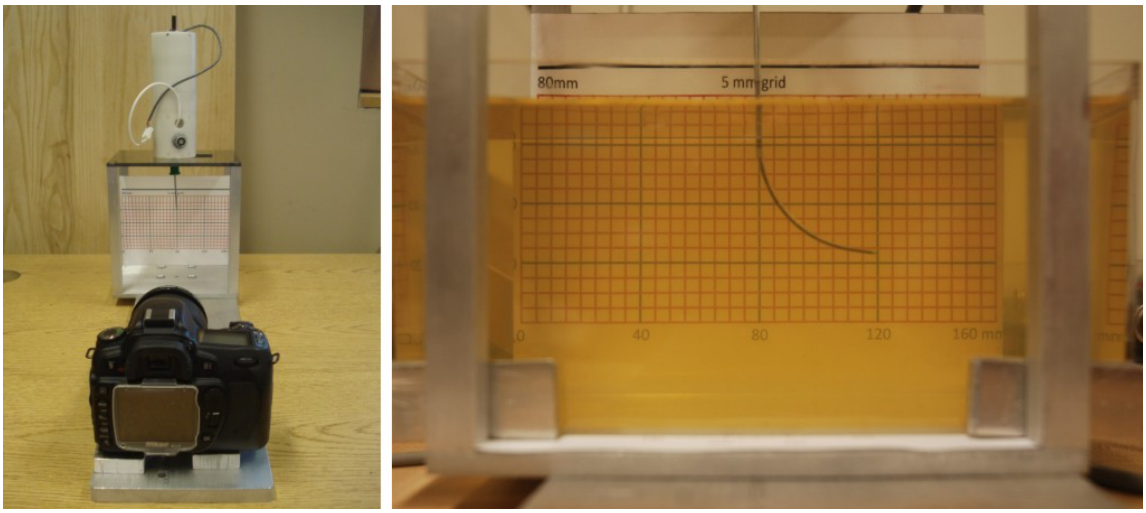

Figure 5. Left, experimental setup showing the camera fixed relative to the test rig. The robot is attached to the top of the test rig and a block of gel can be positioned inside it. Right, a sample image showing the stylet extended from the cannula and into the gel.

The robot mechanism was mounted to the gel box rig, and positioned such that the stylet was deployed in a plane parallel the camera's viewing plane. A grid paper was attached to the back of the gel box rig to provide a coordinate system for making measurements.

The grid as seen through the gel was distorted such that the original square grid (5mm per side) was magnified. Initial experiments with a smaller lens camera also demonstrated significant barrel distortion; however, with the larger lens of the digital SLR camera, this was not found to be a significant problem. In general, the magnification effect of the gel on objects is related to their depth in the gel relative to the camera. Objects in the middle of the gelatin, e.g. the stylet, are distorted a different amount from the grid that is at the back of the gel. Accordingly, the distortion at the point where the stylet was inserted was calibrated according to the grid on the back of the gelatin. This was accomplished using a separate calibration plate made by cutting 10mm square grids into a 1/16in thick aluminum plate. This plate was then placed at the same plane in the gel in which the stylet would be inserted to provide a second frame of reference. This grid was then measured against the grid in the back and a calibration factor was found to relate the size of each grid. The calibration factor was found to be 1.16.

Images were imported into Matlab and a custom script was written that allowed a coordinate systems x and y axis to be specified. Then the script enabled x-y data points in this coordinate system to be recorded by clicking on the stylet tip on the picture. The same reference point was chosen for extracting the data points from each picture. A measurement repeatability error of 0.26 mm was found by taking a stylet tip position measurement five times for two different pictures.

3.2 Experimental Procedure

Six stylets of different radii of curvature and diameter were evaluated through a procedure that involved commanding the stylet distal tip to six different positions in the gel. Before each experiment, a stylet was attached to the device that

was then mounted to the test rig. The gel was placed into the rig, and the cannula was axially translated 15 mm such that the tip of the cannula was about 5 mm inside the gel. A picture was taken to record the distal tip of the cannula and then the stylet was fully deployed and another picture taken and data point recorded. The stylet was then retracted inside the cannula, the cannula translated to 25mm and 35mm positions, and the same stylet motion was repeated at each cannula position. After each cannula and stylet motion, the position of their respective distal tips was recorded. Then the cannula was brought back to the 15 mm position, rotated 180° and a symmetric set of points were targeted as illustrated in Figure 6. This procedure was followed for each of the six stylets of different diameter and radius of curvature.

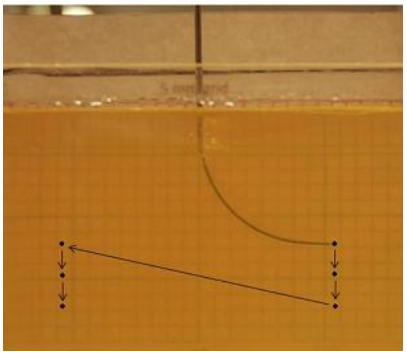

Figure 6. Sequence for targeting the six points in the gel.

3.3 Kinematic Model for Predicting Tip Position

In order to predict the tip location, a kinematic model based on a series of homogeneous transformation matrices (HTM) between coordinate systems assigned to various parts of the device was developed. The locations of the coordinate systems are shown in Figure 7. Each HTM represented some combination of commands send to the cannula and stylet (e.g. translations and rotations), stylet geometry, the angle the stylet exits from the cannula and deflection of the cannula. The position of the distal tip of the stylet with reference to the origin was predicted through the sequential product of all of the HTMs.

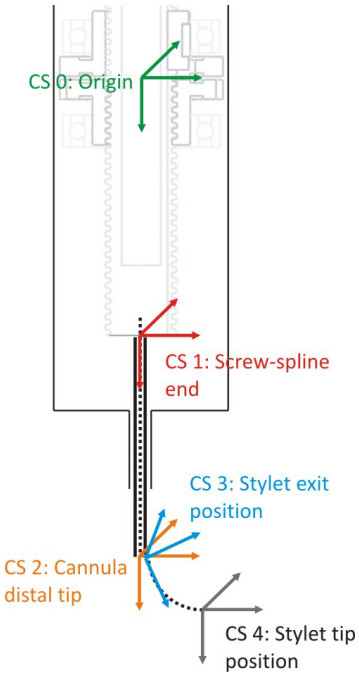

Figure 7. Locations of coordinate systems chosen for kinematic model.

The first HTM is a function of the axial and rotational actuation commands sent to the robot. The tip of the cannula relative to the robot is defined by the axial length of the cannula and the curvature of the cannula induced by the stylet that is inside. Another HTM relates the angle between the cannula axis and a line tangential to the tip of the stylet as it exits the cannula. This angle will always have some finite value as it is necessary to have some clearance between the outside diameter of the stylet and the internal diameter of the cannula. A final HTM relates the stylet tip position relative to the tip of the cannula with its position a function of how far the stylet is commanded to be deployed from the cannula as well as its radius of curvature.

4. RESULTS

A separate picture was taken to record each stylet tip position and this experimental data was compared to that predicted with the kinematic model for each of the stylet geometries. The results of the targeting experiments for the various stylets are shown in Figure 8 along with their specified stylet geometry. The data points near y-axis in each image represent the distal tip of the cannula and the points furthest to the left and right represent the distal tip of the stylet. The experimental and model data are both plotted for each data point.

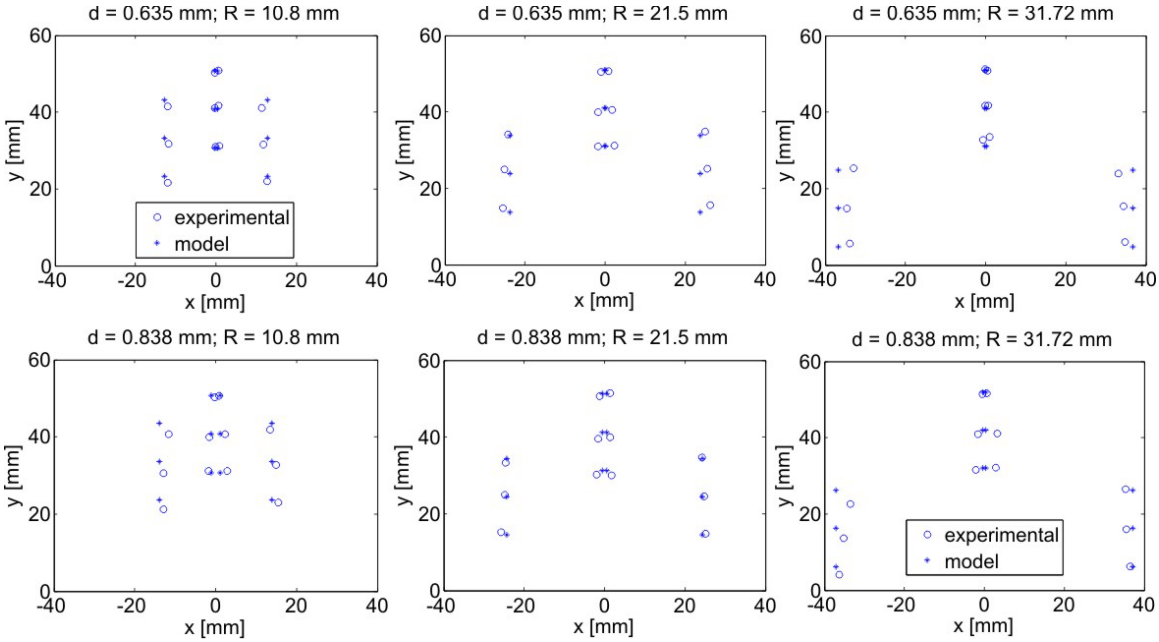

Figure 8. Results from bench level targeting experiments in ballistics gel. This was performed for three different stylet diameters and three different radii of curvature. The experimental and predict stylet distal tip locations are shown.

From Figure 8 it can be seen that there is a reasonable match between the experimental and theoretical data. The difference between the experimental and model data can be seen to be greatest for the positions when the cannula is inserted the greatest amount into the gelatin. Using the estimated parameters, the initial cannula positions of the calculated and measured data were reasonably close for the majority of the different trials. A summary table of the mean and standard deviations of the difference between the experimental data and kinematic model are shown in Table 1.

Table 1. Mean targeting errors for various stylet diameters and radii of curvature

Stylet Geometry	**R = 10.85 [mm]**	**R = 21.55 [mm]**	**R = 31.72 [mm]**
d = 0.635 [mm]	3.34 ± 0.77	1.61 ± 0.61	2.96 ± 2.16
d = 0.838 [mm]	3.26 ± 1.03	1.27 ± 0.72	2.47 ± 1.41

5. CONCLUSIONS AND FUTURE WORK

While catheters have evolved into sophisticated devices that enable physicians to remotely manipulate their tip position, the same level of sophistication has not been applied to for maneuvering medical instruments placed in tissue. The reason for this is that there has previously been no strong medical need for such a tool, but the growing use of energy delivery systems to treat tumors is challenging physicians and engineers to create new delivery means that can extend its use.

In this paper we have presented a preliminary evaluation of a telerobot capable of repositioning the distal tip of a percutaneous instrument, after it has been inserted into a block of ballistics gelatin. The experimental position of the distal tip of the stylet was matched closely to the position predicted by a simple kinematic model successfully demonstrating the concept of robotic needle distal tip repositioning. One interesting observation during the experiments was that as the cannula tip translated downward, the cannula followed a slightly curved path in the tissue due to its slightly curved shape and resultant asymmetric forces on it. This accounted for the larger difference between the experimental data and model. Furthermore, the stylet was also found to deviate slightly from its natural curvature when it was inserted into tissue due to the tangential cutting force at its tip. The amount of stylet deflection will be a function of the stylet geometry (radius of curvature and diameter).

Both the 0.635 mm and 0.838 mm diameter stylets with a radius of curvature of approximately 20 mm were found to have the closest match between theoretical and experimental data. One possible reason for this is that this geometry represented an optimal stiffness. That is, the stylet was stiff enough to not deflect too much when being inserted into tissue and compliant enough so as to not cause significant cannula curvature and thus deflection as it was inserted. Future work is planned to further improve the kinematic model to include a model for stylet deflection in ballistics gelatin and to develop a method for selecting the appropriate stylet and cannula geometry for a given application.

The preliminary experimental data presented in this paper demonstrate the promise of the robotic needle steering instrument that we have developed. For biopsy, an increased targeting capability and an ability to accurately target multiple locations within a single lesion would allow for higher diagnostic rates as well as a reduction in procedure time and radiation dose for the patient. As well as correcting for targeting errors due to instrument deflection or tissue deformation, for the instrument could greatly simplify local treatments such as radiofrequency ablation. Instead of a large diameter probe, or a probe with multiple electrodes, a thin probe with a small burn volume could be inserted into the tumor and then robotically steered so as to raster-scan through the tumor after a single needle insertion through the skin. Such a system might enable treatment to be applied to multiple small but overlapping volumes allowing conformation to the tumor morphology, while avoiding damaging any delicate neighboring tissue. Finer treatment margins as well as the ability to treat multiple tumors, satellite lesions or tumors that cannot be accessed along a straight path are significant advantages of such an approach. Future work is planned to test the device in a realistic clinical setting.

REFERENCES

[1] M. D. Report, [Ablation Technologies Worldwide Market], (2008).

[2] S. N. Goldberg, G. S. Gazelle, C. C. Compton *et al.*, "Radiofrequency tissue ablation in the rabbit lung: Efficacy and complications," Academic Radiology, 2(9), 776-784 (1995).

[3] D. E. Dupuy, R. J. Zagoria, W. Akerley *et al.*, "Percutaneous Radiofrequency Ablation of Malignancies in the Lung," Am. J. Roentgenol., 174(1), 57-59 (2000).

[4] J. M. Lee, G. Y. Jin, S. N. Goldberg *et al.*, "Percutaneous Radiofrequency Ablation for Inoperable Nonâ€"Small Cell Lung Cancer and Metastases: Preliminary Report1," Radiology, 230(1), 125-134 (2004).

[5] K. Steinke, D. Glenn, J. King *et al.*, "Percutaneous pulmonary radiofrequency ablation: difficulty achieving complete ablations in big lung lesions," Br J Radiol, 76(910), 742-745 (2003).

[6] S. N. Goldberg, P. F. Hahn, K. K. Tanabe *et al.*, "Percutaneous Radiofrequency Tissue Ablation: Does Perfusion-mediated Tissue Cooling Limit Coagulation Necrosis?," Journal of Vascular and Interventional Radiology, 9(1), 101-111 (1998).

[7] P. R. Morrison, E. vanSonnenberg, S. Shankar *et al.*, "Radiofrequency Ablation of Thoracic Lesions: Part 1, Experiments in the Normal Porcine Thorax," Am. J. Roentgenol., 184(2), 375-380 (2005).

[8] A. Bzostek, A. C. Barnes, R. Kumar *et al.*, "A Testbed System for Robotically Assisted Percutaneous Pattern Therapy," Medical Image Computing and Computer-Assisted Intervention – MICCAI'99*,* 1679/1999, 1098-1107 (1999).
[9] D. Stoianovici, K. Cleary, A. Patriciu *et al.*, "AcuBot: a robot for radiological interventions," Robotics and Automation, IEEE Transactions on*,* 19(5), 927-930 (2003).
[10] M. Rasmus, S. Dziergwa, T. Haas *et al.*, "Preliminary clinical results with the MRI-compatible guiding system INNOMOTION," Int J CARS 2 (Suppl 1), S138-S145 (2007).
[11] E. Taillant, J.-C. Avila-Vilchis, C. Allegrini *et al.*, [CT and MR Compatible Light Puncture Robot: Architectural Design and First Experiments], (2004).
[12] B. Maurin, B. Bayle, J. Gangloff *et al.*, "A robotized positioning platform guided by computed tomography: practical issues and evaluation." 251-256.
[13] C. Walsh, N. Hanumara, A. Slocum *et al.*, "A Patient-Mounted, Telerobotic Tool for CT-Guided Percutaneous Interventions," ASME Journal of Medical Devices*,* In Press, (2008).
[14] R. H. Taylor, R. H. Taylor, J. Funda *et al.*, "A telerobotic assistant for laparoscopic surgery," Engineering in Medicine and Biology Magazine, IEEE*,* 14(3), 279-288 (1995).
[15] N. Hata, N. Hata, R. Hashimoto *et al.*, "Needle Guiding Robot for MR-guided Microwave Thermotherapy of Liver Tumor using Motorized Remote-Center-of-Motion Constraint." 1652-1656.
[16] E. Boctor, R. r. Webster, H. Mathieu *et al.*, "Virtual remote center of motion control for needle placement robots.," Comput Aided Surg*,* 9(5), 175-83 (2004).
[17] S. P. DiMaio, and S. E. Salcudean, "Needle insertion modelling and simulation." 2, 2098-2105 vol.2.
[18] R. J. Webster, III, J. S. Kim, N. J. Cowan *et al.*, "Nonholonomic Modeling of Needle Steering," Int. J. Rob. Res.*,* 25(5-6), 509-525 (2006).
[19] J. A. Engh, G. Podnar, S. Y. Khoo *et al.*, "Flexible Needle Steering System for Percutaneous Access to Deep Zones of the Brain." 103-104.
[20] R. Ebrahimi, S. Okazawa, R. Rohling *et al.*, [Hand-Held Steerable Needle Device], (2003).
[21] S. Okazawa, R. Ebrahimi, J. Chuang *et al.*, "Hand-held steerable needle device," Mechatronics, IEEE/ASME Transactions on*,* 10(3), 285-296 (2005).
[22] M. Loser, [A new robotic system for visually controlled percutaneous interventions under X-ray or CT-fluoroscopy] Albert-Ludwig-Univ.. Freiburg, Germany(2002).
[23] R. J. Webster, J. M. Romano, and N. J. Cowan, "Mechanics of Precurved-Tube Continuum Robots," Robotics, IEEE Transactions on*,* 25(1), 67-78 (2009).
[24] P. Sears, and P. Dupont, "A Steerable Needle Technology Using Curved Concentric Tubes." 2850-2856.
[25] R. L. Pakter, and E. M. Morris, "Hollow, curved, superlastic medical needle," US Patent No. 6,592,559 B1.
[26] W. R. Daum, "Deflectable Needle Assembly," US Patent No. 6,572,593.
[27] A. Seitel, C. J. Walsh, N. C. Hanumara *et al.*, "Development and evaluation of a new image-based user interface for robot-assisted needle placements with the Robopsy system." 7261, 72610X-9.